Electrochemical Deposition onto Self-Assembled Monolayers
New Insights into Micro- and Nanofabrication

terminal group
(-CH$_3$, -COOH, etc)

hydrocarbon chain

sulphur head

substrate

d)

c)

b)

a)

Defective sites at
alkanethiolate SAM

a)

substrate

Nucleation at
defects of SAM

b)

substrate

Nuclei growth

c)

substrate

Complete coverage of SAM

d)

substrate

Electrochemical Deposition onto Self-Assembled Monolayers: New Insights into Micro- and Nanofabrication

Patricia L. Schilardi,[a] Patricio Dip,[b] Paula C. dos Santos Claro,[a] Guillermo A. Benítez,[a] Mariano H. Fonticelli,[a] Omar Azzaroni,[a] and Roberto C. Salvarezza*[a]

Abstract: Pattern transfer with high resolution is a frontier topic in the emerging field of nanotechnologies. Electrochemical molding is a possible route for nanopatterning metal, alloys and oxide surfaces with high resolution in a simple and inexpensive way. This method involves electrodeposition onto a conducting master covered by a self-assembled alkanethiolate monolayer (SAMs). This molecular film enables direct surface–relief pattern transfer from the conducting master to the inner face of the electrodeposit, and also allows an easy release of the electrodeposited film due their excellent anti-adherent properties. Replicas of the original conductive master can be also obtained by a simple two-step procedure. SAM quality and stability under electrodeposition conditions combined with the formation of smooth electrodeposits are crucial to obtain high-quality pattern transfer with sub-50 nm resolution.

Keywords: alloys · electrochemistry · metal · nanotechnology · oxides · self-assembled monolayers

Introduction

Design and development of novel and reproducible strategies for nanopatterning surfaces became one of the most relevant topics involved on the progress of nanotechnology[1] However, in many cases, interesting patterning approaches were not able to reach the presumed technological impact as a consequence of lacking the required combination of re-

[a] Dr. P. L. Schilardi, P. C. dos Santos Claro, Dr. G. A. Benítez,
Dr. M. H. Fonticelli, Dr. O. Azzaroni, Dr. R. C. Salvarezza
Instituto de Investigaciones Fisicoquímicas
Teóricas y Aplicadas (INIFTA)
Facultad de Ciencias Exactas
Universidad Nacional de La Plata - CONICET
Sucursal 4 Casilla de Correo 16 (1900) La Plata (Argentina)
Fax: (+54) 221-425-4642
E-mail: robsalva@inifta.unlp.edu.ar

producibility, accuracy, simplicity and more important, suitability for large-scale fabrication. One breakthrough on the development of alternative nanofabrication techniques was brought by "soft lithographic techniques" initially developed by Whitesides' group at Harvard University about a decade ago.[2] Soft lithography is a set of techniques that rely on molding with rubber (polydimethylsiloxane, PDMS), silicon or quartz stamps to make micro- and nanostructures. In general, molding techniques are particularly attractive because they are relatively simple, low cost and suitable for large-scale fabrication.

A crucial point for the use of molding techniques is the adherence between the material to be patterned and the master. The adherence should be extremely low in order to allow the release of the deposited material without damaging the master or the molded surface. This is commonly achieved by the use of anti-adherent layers such as Teflon-like coatings or oxides and sulfides films,[3] but in these cases the size of the features that can be transferred is limited by the surface roughness of the anti-sticking layer. The other problem when handled with rigid materials is the surface roughness of the deposit that also limits the resolution of the pattern transfer process. Therefore, molding techniques in the nano/microscale have been mainly limited for direct patterning polymeric materials with a relatively low adherence using rubber (PDMS), silicon or quartz stamps.[2] Under this perspective, the development of new routes for direct nano/micropatterning of metals, alloys, oxides, semiconductor and ceramic surfaces by molding techniques should be a technological goal with immediate impact in mass-production processes such as CDs, DVDs, solar cells or magnetic devices.

Our strategy to extend the molding concept for nano/micropatterning to a wide range of materials and a broad spectrum of deposition techniques was the use of metallic or semiconductor masters modified with molecular film as anti-adherent layer,[4,5] in particular alkanethiolates and silanes self-assembled monolayers (SAMs). On the other hand, the problem related to the surface roughness of the deposited

materials was managed by using high deposition rates that produces nanometer sized grains, and in some cases by the addition of organic additives.[6]

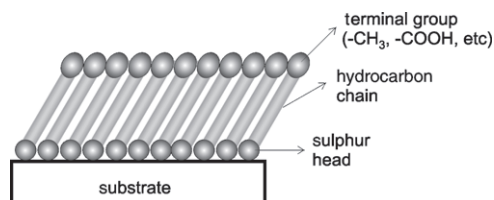SAMs can be described as single layer of highly oriented, ordered and packed molecules adsorbed on a substrate
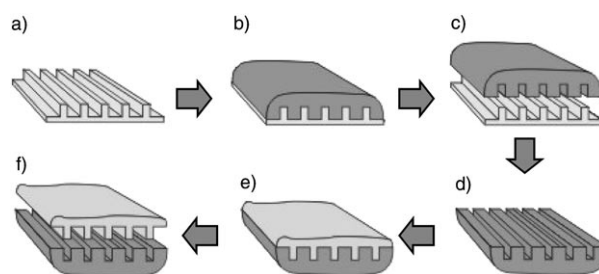

Figure 1. Alkanethiolate SAM: Lateral view.

Figure 2. a) Alkanethiolate covered master; b) deposition step; c) release step, the inner face of the deposit is a mold of the master; d) alkanethiolate covered mold; e) deposition step; f) release step, the inner face of the deposit is a replica of the master shown in a). As the alkanethiolate SAMs remains on the master or mold surface after release they can be reused for the preparation of new molds or replicas.

through a strong covalent bond. Among them, SAMs of alkanethiols (Figure 1) on metals[7,8] and silanes on oxidized surfaces[8] have been extensively studied because they provide a route to control corrosion, they serve to anchor different functional groups that are used to detect molecules and biomolecules in sensors and biosensors, they are crucial components in nanodevices for electronics, and finally because they provide an easy method to create well-defined surfaces with controllable chemical functionality. In this way wetting, lubrication and adhesion properties of solid surfaces can be easily modified.

In fact, it is well known that when the terminal group of thiolate or silane SAMs is a methyl group the adherence of different types of materials (rigid polymers, metals, ceramics, oxides) to the SAM-covered substrate is dramatically reduced.[4,5,9] Thus, there has been general agreement that a proper ω-fuctionalization of the thiols is required in order to metallize thiolate SAMs on metals,[10] an important issue in molecular electronics and spintronics. Other interesting property of SAMs is that, conversely with other antisticking agents, they exhibit an extremely low roughness that arises from molecular defects.[11] In fact, the defect size and defect height, are well below the sub-50 nm, the current frontier in nanotechnology. With this scenario in mind it is clear why alkanethiolate SAMs can be used as key agents for pattern transfer with nanoscale resolution. The procedure that we have used is quite simple as shown in Figure 2.

The master is immersed in a solution containing the alkanethiol or silane molecules to form the self-assembled monolayer. Subsequently, a metal, ceramic or semiconductor material is deposited. Finally, after a preset thickness is reached the deposit is released from the substrate. In this fashion (Figure 2 a–c) the surface of different materials has been nano/micromolded: metals by using thermal vapor deposition (PVD),[5] ceramics by reactive sputtering,[12] and semiconductors by laser ablation.[13] If the procedure is repeated (by functionalized the mold) a replica of the master can be obtained in a simple way (Figure 2d–f). From the point of view of the deposition process itself there are two key points to obtain pattern transfer with nanoscale resolu-

tion. The first one is the stability of the self-assembled monolayers under deposition conditions, particularly substrate temperature and the energy of incoming particles (ions, molecules). The second one is that the depositing material must follow closely the surface topography of the master without the triggering of instabilities, that is, a conformal growth to the master is needed during the deposition process.

Electrochemical Molding: A New Route for Metals and Metal Oxides Nano/Micropatterning

In principle, the extension of the procedure described in Figure 2 for nano/micropatterning metals and oxides by electrodeposition appears simple and particularly attractive. In fact, metal electrodeposition is a well known technique involving relatively low cost equipments accessible to all chemistry laboratories, and it is currently used in many technological applications. Electrodeposition is used to produce materials and architectures that can not be built by traditional techniques. By means of this method a variety of materials such as nanocomposites, epitaxially deposited metal films, compositional superlattices and ceramic materials have been produced.[14] The extension of the method described in Figure 2 for the electrochemical nano/micropatterning of metal and oxides requires answering some important questions: 1) Are SAMs on metallic masters stable under electrodeposition conditions? 2) Are defect size and defect density of the molecular films in the plating bath compatible with a large scale pattern transfer? 3) Are grain size and roughness of the metal or oxide films resulting from electrodeposition on SAMs-covered masters compatible with nano/microscale features? In the next we will discuss these issues and answer these questions.

SAMs Preparation and Quality

SAMs can be prepared from the gas phase or by solution preparation by a wet route through immersion of clean Au

or Ag substrates in alkanethiolate containing solutions.[7,8] In both cases the following reaction has been proposed for the self-assembly process:

$$CH_3\text{-}(CH_2)_n\text{-}H_2C\text{-}SH + Me$$
$$\rightarrow CH_3\text{-}(CH_2)_n\text{-}H_2C\text{-}S\text{-}Me + {}^1\!/_2 H_2 \tag{1}$$
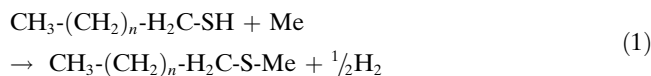
where Me stands for the metal substrate. Due to the low solubility of alkanethiols in water the procedure involves the use of ethanol, benzene, toluene or hexane as solvents. Examples of ordered alkanethiolates SAMs on Ag and Au surfaces formed by simple immersion of clean metal surfaces in
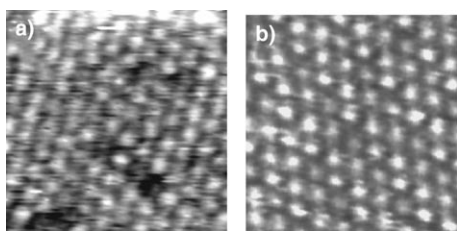

Figure 3. a) 4.5×4.5 nm^2 STM image (top view) with molecular resolution showing $\sqrt{7} \times \sqrt{7}$ $R19.1°$ propanethiolate lattice on Ag(111); b) 4.5×4.5 nm^2 STM image of the $\sqrt{3} \times \sqrt{3}$ $R30°$ hexanethiolate lattice on Au-(111). Note the presence of some vacancies (molecular defects) in Figure 3a. Solutions: 5 μM alkanethiol containing ethanolic solutions, immersion times: 24 h, $T = 25$ C.

ethanolic solutions for 24 h are shown in Figure 3.

Oxidized Cu surfaces can also form ordered self-assembled alkanethiolate monolayers. In fact, a redox reaction takes place during immersion between the copper oxides and the alkanethiolate molecules yielding metallic Cu and alkanesulfonates.[15] As the oxide is reduced the clean Cu atoms react with the alkanethiolate molecules yielding ordered monolayers. For self-assembly on Cu surfaces benzene, toluene or hexane are preferred. Self-assembly of alkanethiols on oxidized metals such as Fe and Ni is more difficult.[16,17] In both cases to obtain good quality SAMs the oxide must be completely removed. Some methods have been developed for these purposes, one of them first involving the metal-oxide electroreduction followed by sample immersion in a non-aqueous solution containing the alkanethiol molecules.[18] In the case of oxidized Ti, Al or silicon surfaces, silane molecules form covalent bonds through OH surface species leading to molecular films.[8] Substrate immersion in silane-containing solutions in dry hexane is mandatory to obtain good quality silane SAMs. The formation of ordered alkanethiolate and silane monolayers normally involves immersion times ranging from 4–24 h, depending on the hydrocarbon chain length. In both cases, alkanethiolate and silane SAMs, at high surface coverage the molecules adopt a nearly vertical configurations.[7,8]

Alkanethiolate lattices contain, however, different types of defects[11] such as missing rows (Figure 4a), molecular defects (Figure 3a, 4b) where the molecules are absent or dis-
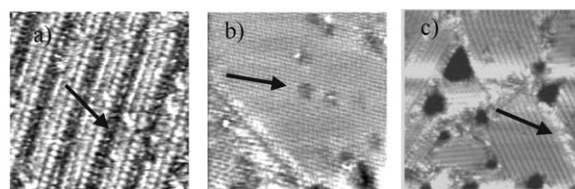

Figure 4. Typical defects at SAMs (arrows). a) 11.5×11.5 nm^2 STM image. Missing rows of propanethiolate molecules at a SAM on Au(111); b) in situ 20×20 nm^2 STM image. Molecular defects at a $\sqrt{3} \times \sqrt{3}$ $R30°$ hexanethiolate lattice on Au(111), electrolyte: NaOH (0.1 M), applied potential $E = -0.7$ V vs the saturated calomel electrode (SCE); c) 35×35 nm^2 STM image. Domain boundaries in hexanethiolate–Au(111) c-(4×2) lattices. Large black regions are not true SAMs defects as explained in the text.

ordered, and domains boundaries, where the alkanethiolate molecules exhibit strong disorder (Figure 4c). The black large islands in Figure 4c are not real SAMs defects.[19] They are holes, monoatomic (0.24 nm) or diatomic (0.48 nm) in depth, formed during the self-assembly process. The hole bottoms are also covered by the alkanethiolate molecules.[19]

The size and height (the thickness of the SAM) of these defects limit the resolution that can be achieved, that is, the minimum size of the features that can be transferred from the master to the deposited material.

The stability under ambient conditions is also an important variable when handling with SAMs. It has been shown that the rate of degradation, for instance oxidation to alkanesulfonates, increases rapidly with decreasing alkyl chain length.[20] Furthermore, for short-chain alkanethiol SAMs with $n = 3$, a randomly initialized degradation plays a major role, whereas for long-chain alkanethiol SAMs, the degradation starts at domain boundaries and defects, propagating into intact domains. Thus, the importance in growing large alkanethiolate domains in order to reduce domain boundaries clearly emerges. We have used hexanethiolate and dodecanethiolate SAM-covered metals for several days without observing significant degradation.

Electrochemical Stability of SAMs

The stability of SAMs in aqueous electrolyte is a crucial point for the application of the electrochemical molding method shown in Figure 2. It is well known that SAMs of alkanethiolates on Au, Ag and Cu exhibit reductive electrodesorption[21] according to the following reaction:[22]

$$R\text{-}S\text{-}Me + e^- \rightarrow RS^- + Me \tag{2}$$

where R-S-Me stands for the adsorbed alkanethiolate. In fact, the typical current (j) potential (E) profiles recorded in an electrochemical cell for a alkanethiolate-covered Au (or Ag) substrate in alkaline solutions exhibit well defined current peaks (Figure 5a) related to Reaction (2). Peak labeled as CI corresponds to the reductive electrodesorption reaction while peak AI corresponds to the oxidative electroad-
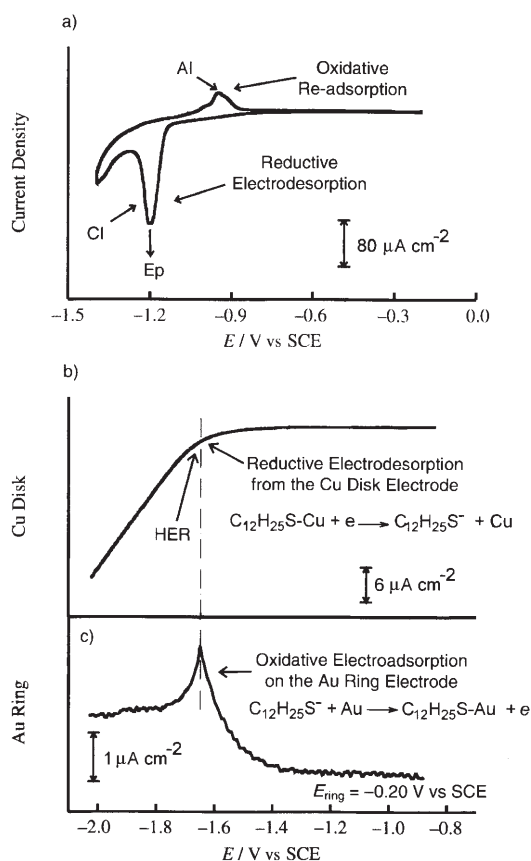
a)

Figure 5. a) Typical current density vs potential profile recorded for a do-decanethiolate–SAM on Au(111) in 0.1 M NaOH. The potential scan starts in the negative direction. The electrodesorption peak, peak potential (E_p), and oxidative readsorption peak are indicated. b) Typical current density vs potential profile recorded for a dodecanethiolate–SAM on a rotating Cu electrode in NaOH (0.1 M) $+$ H$_2$O (5%) in methanol. No evidences of alkanethiol electrodesorption are observed due to HER. c) Ring current at the Au ring showing oxidative adsorption when alkanethiolates are desorbed from the rotating Cu disc b).

sorption of molecules produced at CI. The charge density (q) involved in peak CI is that expected for desorption of a complete monolayer of the ordered lattices ($q \approx 0.080$ mC cm^{-2}) shown in Figure 3. In situ STM images have been shown that the SAMs structure remains practically unaltered for applied potentials more positive than those corresponding to peak CI,[11b] that is, preceding SAMs desorption. Therefore, the peak potential (E_p) (arrow in Figure 5a) has been widely used to test the stability of the SAMs against reductive electrodesorption.[23]

In the case of Cu, the E_p measurements are more difficult because SAMs electrodesorption takes place simultaneously with the hydrogen evolution reaction (HER) (Figure 5b). In this case, the rotating disc-ring technique has been used for the E_p determination.[24] The electrode consisted in a alkanethiolate-covered Cu disc and Au ring. The ring potential was held at -0.2 V so that when the applied potential to the Cu disc reaches E_p, the desorbed alkanethiolates [Reaction (2)] are electroadsorbed on the Au ring [Reaction (1)] leading to

a detectable positive (anodic) current (Figure 5c).[25] Note that HER takes place as the SAM is electroreduced, that is, as free Cu sites are produced.

The reductive electrodesorption [Reaction (2)] depends on the electrolyte pH (Figure 6a–d). While E_p remains
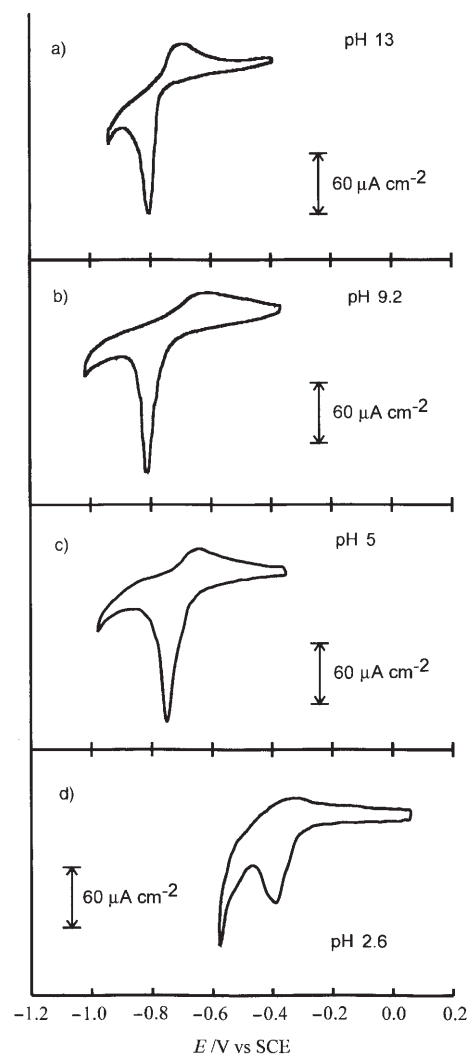
Figure 6. Current vs potential profiles recorded for a Au(111) electrode at 0.05 V s^{-1} in electrolyte solutions containing 5 μM propanethiol at different pH values. The electroadsorption/electrodesorption peaks shift only in relatively strong acid media.

nearly constant in the $3 < \mathrm{pH} < 14$ range, it moves in the positive direction for pH values lower than 3, that is, alkanethiolates are less stable in strong acid media.[21,26]

In Figure 7 E_p vs n, the number of C atoms in the alkanethiol chain, for Au in acid (pH <3) and alkaline solutions (pH 13) are plotted. From Figure 7 it is evident that SAM stability increases with n, due to the increase in van der Waals interactions between the hydrocarbon chains and hydrophobic forces between the molecules and water.[23] In acid media the E_p versus n plot results in a straight line with
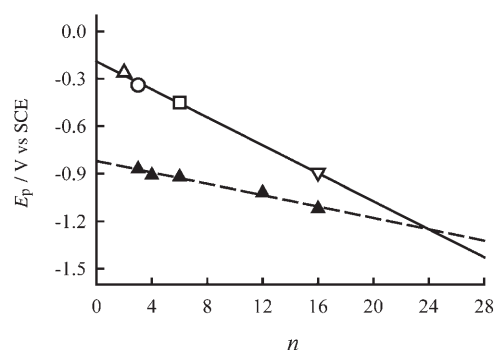
Figure 7. E_p vs n, the number of C units, for SAMs electrodesorption from Au substrates in 0.1 M NaOH (pH 13, dashed line) and acidic media (pH < 3, continuous line). Open symbols: (△) current vs potential profiles, from reference,[22] (○) current vs potential profiles, (□) current vs potential profiles, from ref. [27], (▽) rotating ring-disc technique.

slope 4 kJ mol^{-1} per carbon unit, which is about 1 kJ mol^{-1} per carbon unit higher than that observed in alkaline solutions. In fact, the lower solubility of alkanethiolate molecules in acid media is an additional factor that stabilizes SAMs against desorption. However, for a given thiolate the E_p value in acid media is always more positive than that measured in alkaline solutions,[26] that is, alkanethiolate SAMs are more stable in alkaline solutions. On the other hand, for a constant n the stability of alkanethiolates increases in the following order Au < Ag < Cu (Figure 8).[24]
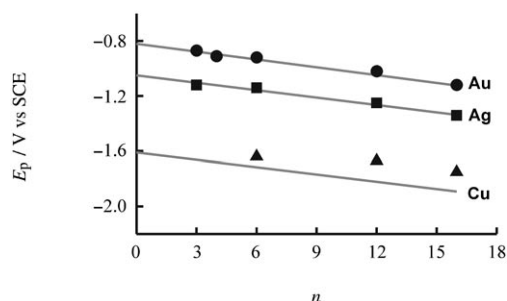

Figure 8. E_p vs n, the number of C units, for alkanethiolates electrodesorption from different substrates. Electrolyte: NaOH (0.1 M) + H$_2$O (5%)in methanol. The solid lines correspond to the theoretical lines estimated by the model reported in ref. [24].

Density functional theory calculations[24] have shown that the electrodesorption potential for a given alkanethiol on different metals results from a balance between the adsorption energy of the organic molecule on the metal surface (which varies in the 40–60 kcal mol^{-1} range), the energy to introduce an electron into the alkanethiolate–metal system, and the solvation of the metal surface.

Finally, it should be also noted that the plating bath temperature is not an important variable as alkanethiols on metals are stable up to 100 C.[28]

From the above discussion the importance of the alkanethiol length (n), substrate and pH on electrochemical nanopatterning clearly emerges. For instance alkaline plating baths should be preferred to acid baths due to the higher stability range. SAMs on Cu masters should exhibit greater stability range than those on Au masters, in both alkaline and acid media. Longer alkanethiols should be preferred to the shorter ones due to their higher stability induced by van der Waals and hydrophobic interactions. However, as already mentioned SAM thickness limits the vertical resolution of method so that alkanethiols with an intermediate number of C (typically n = 12) should be used. On the other hand, the advantages of Au master for nanoscale patterning are evident: alkanethiolate SAMs on Au are more crystalline and ordered than those formed on Cu and Ag thus reducing the defect density and size.

Metal electrodeposition on SAMs covered substrates: When the electrodeposition is performed at relatively high rates on SAMs covered metal electrodes[29] the first step is the nucleation of the deposited material at defective sites of the molecular film (Figure 9a, b). This stage is followed by the growth of the nuclei within these defects towards the SAMs/electrolyte interface (Figure 9c). Finally, when the nuclei reach the outer plane of the SAM, three-dimensional growth takes place leading to a complete coverage of the alkanethiolate film by a metal or oxide layer (Figure 9d). Conversely, when Ag is electrodeposited on SAM-covered Au at a low rate a place exchange mechanism has been observed.[27] In fact, depending on the relative adsorption energies and deposition rate alkanethiolate species have time to desorb from the substrate and re-adsorb on the depositing
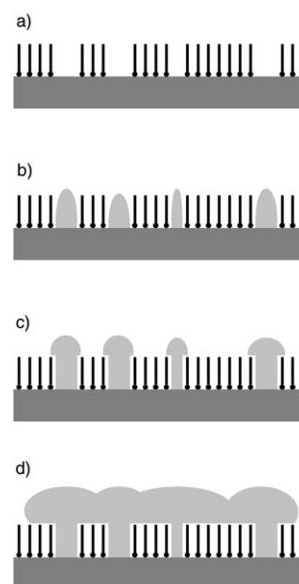

Figure 9. Scheme showing the steps involved in metal electrodeposition on SAMs covered substrates. a) Defective sites at SAMs (the molecules are indicated in black); b) nucleation and growth of the metal (grey) within the SAM; c) three dimensional growth outside the SAM; d) formation of a continuous metallic film on the SAM.
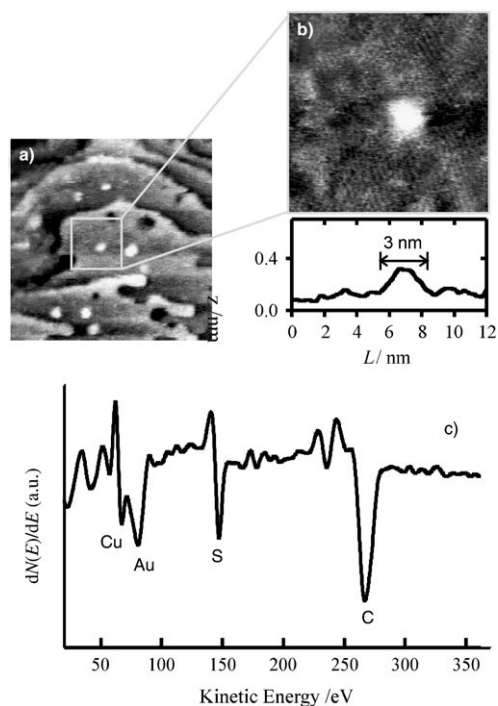
Figure 10. STM images and AES data taken at the early stages of Cu electrodeposition on propanethiolate-covered Au(111). a) 45×45 nm^2; b) 12×12 nm^2 high resolution of an individual Cu cluster. The rows of propanethiolates molecules are also observed around the cluster. The cross section indicates that the deposition process is at stage c) of Figure 9. AES analysis showing Cu, S and C signals corresponding to the Cu electrodeposit, and the propanethiolate SAM (S, C). Plating bath: CuSO$_4$·5H$_2$O (0.6 M) + H$_2$SO$_4$ (0.5 M) + thiourea (0.025 mM), plating bath temperature $T = 25$°C.

metal. Thus, the SAM floats during deposition turning the method described in Figure 2 inapplicable.

The mechanism shown in Figure 9 is strongly supported by experimental data. STM images (Figure 10a, b) and Auger electron spectroscopy data (Figure 10c) taken at the early stages of Cu electrodeposition on a propanethiolate covered Au (that correspond to stages b–c in Figure 9) reveal the presence of few nanometer-sized Cu clusters (3–5 nm diameter, 0.3 nm in height).

These clusters are formed at the nanometer-sized defects present at alkanethiolate SAMs as previously discussed. At advanced stages complete metallization of the alkanethiolate-covered gold electrode is observed. Depending on the electrodeposition time nanometer or micrometer-thick metal films can be grown on SAMs covered substrates. It is evident that the deposited films are connected to the substrate only by the small metal clusters shown in Figure 9. The number of connections depends on the defect density that in turn decreases markedly with the number of C units in the hydrocarbon chains. For instance, dodecanethiolate–SAMs exhibit not only a wide stability range against desorption (Figure 7) from the Au surface but also smaller defect density than propanethiolate–SAMs.[11] However, it should be noted that a determined population of defects is required in order to electrodeposit the metal film on the SAM-cov-

ered substrate. In other words, we need a defect density enabling an efficient flow of current in order to completely metallize the sample. Nevertheless, this population should be small enough to allow pattern transfer in the nanometer scale and easy detachment without damaging the master or the film.

Figures 9 and 10 also show two other possible applications of this method. The first one (stages b–c) is related to the preparation of metallic clusters on foreign substrates by a confined growth process (at the SAM defects). The second one (stage c) is for fabricating nanocontacs between two metallic electrodes.

The release step (Figure 2c) involves the rupture of the metallic nanocontacts between the substrate and the deposited film. Thus, the height of these contacts, which in turn are determined by the thickness of the molecular film, introduces a surface roughness that limits the vertical resolution. On the other hand, the size of defect and defect density influence the lateral resolution and also can restrict large scale patterning of the deposited surface. In the case of alkanethiolate SAMs the thickness can be easily varied by changing the number of C units (n) in the hydrocarbon chain, for instance for dodecanethiolate SAMs on Au the film thickness is ≈ 1.7 nm. Therefore, from the point of view of defects long alkanethiolate are good candidates for nanopatterning because they exhibit a lower defect density and smaller defect size, thus improving the lateral resolution of the pattern transfer method. For instance, one should expect that the resolution limits of the pattern transfer method introduced by a SAM of dodecanethiolate itself should be in the order of 5 nm lateral and 2 nm vertical.

In the case of the bare electrode surface, the energy involved in the release step of the electrodeposit from the substrate is close to the Cu/Au cohesion energy, 3.81 eV.[30] When electrodeposition is carried out in presence of SAMs the connectivity between the substrate and the deposit is only given by the electrocrystallization nuclei grown at SAM defects. These nuclei are responsible to keep the electrodeposit attached to the substrate. The interaction between the deposited metal film and methyl-terminated SAM is mainly governed by dispersion forces, which are quantitatively much weaker than metallic bonds associated to Cu/Au cohesion. Thus, the required work to release an electrodeposited film from a substrate (the adhesion work, W_{adhes}) is dramatically decreased as the real metal–metal contact area is reduced. In the case of dodecanethiolate–SAMs we have estimated the uncovered area (the contact area) in 0.01% from electrochemical measurements.[31] This fact implies that in presence of the SAM, the effective cohesion energy corresponding to the electrode–SAM–electrodeposit is 100 times smaller than that corresponding to the electrode-electrodeposit system.

Concerning to this key issue, it must be noted that the actual energy involved on peeling-off the electrodeposited film (W_{peel}) is higher than the adhesion or cohesion work as a consequence of energy dissipation effects during the fracture of the interface.[32]

Notwithstanding, in accordance to the classic peel-off adhesion model exists a direct correlation between the resistance to the fracture of the interface and the adhesion energy.[33] Thus, W_{adhes} can be considered as a reliable parameter proportional to the resistance to the fracture of the electrode-electrodeposit interface. In addition, it is well known that W_{adhes} is proportional to the surface energy of the substrate, γ_{surf}:

$$W_{peel} > W_{adhes} \propto \gamma_{surf} \qquad (3)$$

SAM-covered substrates can be described as binary surfaces with covered and uncovered domains. In the case of copper electrodes, the uncovered and SAM-covered domains have surface energies γ_{Cu} and γ_{SAM}, respectively. Assuming a linear combination on γ_{surf}, we obtain

$$\gamma_{surf} = \theta_{SAM}\gamma_{SAM} + \theta_{Cu}\gamma_{Cu} \qquad (4)$$

where θ_{Cu} and θ_{SAM} are the fraction areas corresponding to the bare and SAM-covered domains. Thus, $\gamma_{SAM} = 29\ mN\,m^{-1}$[34] and $\gamma_{Cu} = 900\ mN\,m^{-1}$[35] gives:

$$\gamma_{surf} = 0.99 \times 29\ mN\,m^{-1} + 0.01 \times 900\ mN\,m^{-1} = 37.7\ mN\,m^{-1}$$

It means that the W_{peel} required for the release of a Cu film from a dodecanethiol-covered substrate is $\approx 1/25$ smaller than that needed to release a Cu film from a bare surface.

Therefore, an electrodeposited Cu film can be easily detached from the SAM-covered master by using tweezers or a scotch tape introducing damages neither to the Cu film nor to the master surface.

Kinetics aspects of metal electrodeposition on SAMs covered substrates: Typical current density (j)/potential (E) profiles for Cu electrodeposition on uncovered and dodecanethiolate-covered Au surfaces from an acid plating bath are shown in Figure 11.

The j versus E profiles show that an alkanethiolate SAM on Au strongly hinder Cu electrodeposition, that is, in the
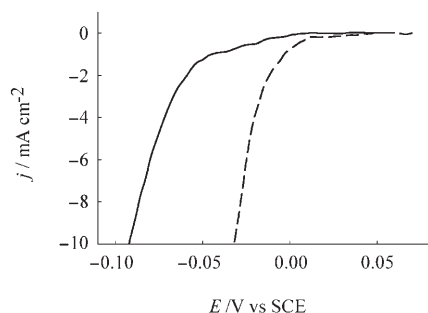
Figure 11. Current (j) vs potential (E) profiles recorded for Cu electrodeposition on Au(111) (-----) and dodecanethiolate covered Au(111) (——) from CuSO$_4$·5H$_2$O (0.6 M) + H$_2$SO$_4$ (0.5 M) + thiourea (0.025 mM), plating bath temperature $T = 25\,°C$.

presence of SAMs we should apply a larger negative potential to obtain a preset current density.[29] In fact, the number of Au sites available for Cu nucleation on a SAM-covered Au electrode is too smaller than that present in uncovered Au surfaces (Figure 10), thus the nucleation rate is markedly reduced. In addition, to form Cu nuclei at Au sites Cu ions should diffuse and/or migrate through a highly hydrophobic environment. The presence of overpotentials originated by the SAMs are important because the magnitude of the negative potential reached by the system under typical galvanostatic conditions determines either SAM stability or desorption (Figures 7, 8), and, accordingly, the applicability of the method shown in Figure 2.

Electrodeposit quality and pattern transfer: In general the lateral and vertical resolutions of pattern transfer methods based on deposition techniques should depend on grain size (d) and roughness of the deposited films. It has been shown that the dynamic scaling of growing interfaces[36] becomes a suitable approach to analyze this problem. Here, the root mean square roughness (W) depends on the deposition time (t) and sample size (L) according to

$$W \approx t^{\beta} \qquad (5)$$

$$W \approx L^{\alpha} \qquad (6)$$

$$d \approx t^{1/z} \qquad (7)$$

$$\frac{1}{z} = \beta/\alpha \qquad (8)$$

where α, β and z are the roughness, growth and dynamic exponents, respectively. For the inner electrodeposit face (that in contact with the alkanethiolate-covered master) the electrodeposition time $t \to 0$, thus from Equations (5) and (7) $W \to 0$ and $d \to 0$. It means that the inner face of the deposit exhibits the best conditions in relation to grain size and roughness. On the other hand, Equation (6) tells us about the restrictions for large scale patterning as W increases with the system size. Smaller α and β values imply a better quality for the deposit, and also a good tendency to produce conformal deposition.[37] In general organic additives must be added to the plating bath in order to obtain stable interfaces with low α and β values.[6,38] The presence of the organic additives avoids the triggering of instabilities during electrodeposition leading to smooth surfaces with nanometer sized grains.

Pattern transfer in the sub-micrometer scale: We demonstrate the applicability of electrochemical soft-lithography to built surface-relief structures in the sub-micrometer range by fabricating a soft-magnetic alloy (Fe$_{11}$Co$_{38}$Ni$_{51}$) grating[39] from a complex plating bath.[40] In order to obtain good deposit with nanometer-sized grains and small roughness the electrodeposition process should be performed at relatively high current densities, that is, $j = 20\ mA\,cm^{-2}$. Under these conditions the substrate reaches potential values close to

−1.2 V. Therefore, a dodecanethiolate-covered Cu master was selected due to its stability at high negative potentials. In this case we have used a Cu master that exhibits a periodic array (Figure 12a) with 1.6 μm wavelength (L).
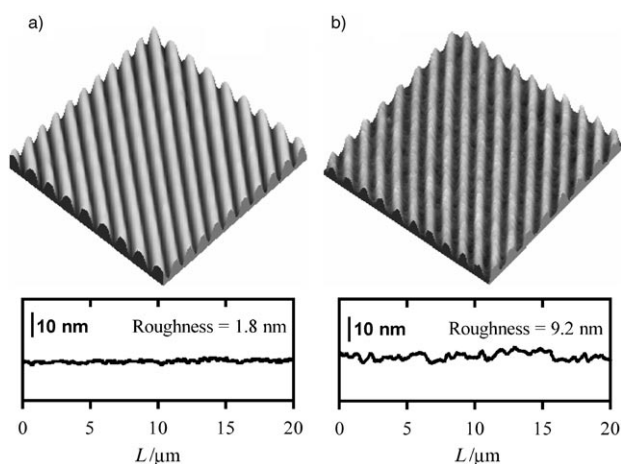

Figure 12. 20×20 μm^2 AFM images (top) and section (bottom) of a) dodecanethiolate-covered Cu master; b) inner face of $Fe_{11}Co_{38}Ni_{51}$ electrodeposit grown at $j = 20$ mA cm^{-2} from $CoSO_4 \cdot 7H_2O$ (0.06 M) + $NiSO_4 \cdot 6H_2O$ (0.2 M) + $FeSO_4 \cdot 7H_2O$ (0.015 M) + NH_4Cl (0.028 M) + H_3BO_3 (0.4 M) + thiourea (2.6×10^{-4} M), pH 2.8.[40]

The root mean square roughness of the master (W) measured parallel to the channels direction was close to 2 nm (Figure 12). The master was immersed in a dodecanethiol-containing toluenic solution (50 μM) for 12 h in order to allow the self-assembly of the dodecanethiolate species on the Cu surface. Then, the procedure described in Figure 2 was followed. After depositing a 10 μm thick alloy film on the dodecanethiol functionalized Cu the alloy film was detached from the Cu master with tweezers. The AFM images of the inner face of deposited alloy (Figure 12b) show a good quality "mold" of the Cu master microstructure. The W value also measured parallel to the channels direction is now 9.2 nm (Figure 12b), that is, an increase in roughness takes place during the pattern transfer. However, this increase is not too important when compared to the height of the relief structure (90 nm).

This method can be also used for patterning oxides surfaces in the submicrometer scale. As an example we show results for pattern transfer to a Cu_2O film. The oxide film was deposited on an alkanethiolate-modified Cu master similar to that depicted en Figure 12a (but $L = 780$ nm) from a plating bath developed by Switzer et al.,[41] and applying a constant potential value at the electrochemical interface ($E = -0.45$ V).

Again, after detachment the AFM image (Figure 13a–b) shows the accurate manner in which the surface structures have been transferred from the Cu master to the oxide film. Similar results were obtained in our Laboratory for electro-

deposited ZnO films indicating that the electrochemical molding method can be extended to other oxides.

Pattern transfer in the nanoscale: Pattern transfer in the nanoscale requires ordered and crystalline SAMs with a low defect density and defect size. Therefore, Au masters are the best candidate for this purpose. A typical Atomic Force Microscopy (AFM) image of an Au surface used as a master is shown in Figure 14a.
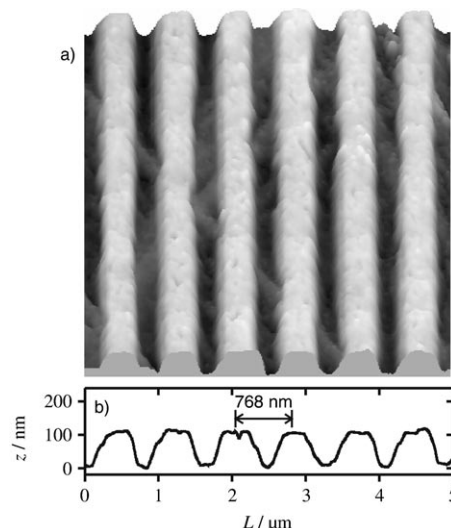

Figure 13. 5×5 μm^2 AFM images (top) and section (bottom) of a patterned Cu_2O film taken after the release step from a Cu master. The film was electrodeposited from $CuSO_4 \cdot 5H_2O$ (0.4 M) + lactic acid (3 M) pH 9 at $T = 60$ °C.[41]

The surface exhibits an hexagonal array of short-range ordered nanoholes with a hole density $\approx 10^{11}$ cm^{-2}. The power spectral density (PSD) from different images indicates that the size of the nanoholes is 50 ± 2 nm while the cross section (Figure 14a cross section) show that the nanohole depth is 3 ± 0.5 nm. The W value measured on 1 μm^2 images results in $W = 0.8$–1.0 nm The Au master was then covered by a dodecanethiol SAM, and used as the working electrode for Cu electrodeposition at 10 mA cm^{-2} from an acid bath containing thiourea as additive.[4,6]

After electrodeposition of the Cu film (≈ 10 μm in thickness) and film release AFM images of the Cu surface in contact with the SAM-covered Au master were taken. These images (Figure 14b) show a patterned Cu surface consisting of arrays of dots with short range hexagonal order as expected for a negative of the master surface. The corresponding cross-sections show the accurate way in which the master features (Figure 14a) have been transferred to the Cu surface (Figure 14b). In fact, Cu dots are 51 ± 2 nm in size (from the PSD analysis) and 2 ± 0.5 nm in height, both figures in well agreement with those measured on the master surface. The W value of the patterned (dots) Cu deposit measured from 1 μm^2 in size AFM images is very low $W = 1.2$–1.6 nm, however slightly higher than that measured for
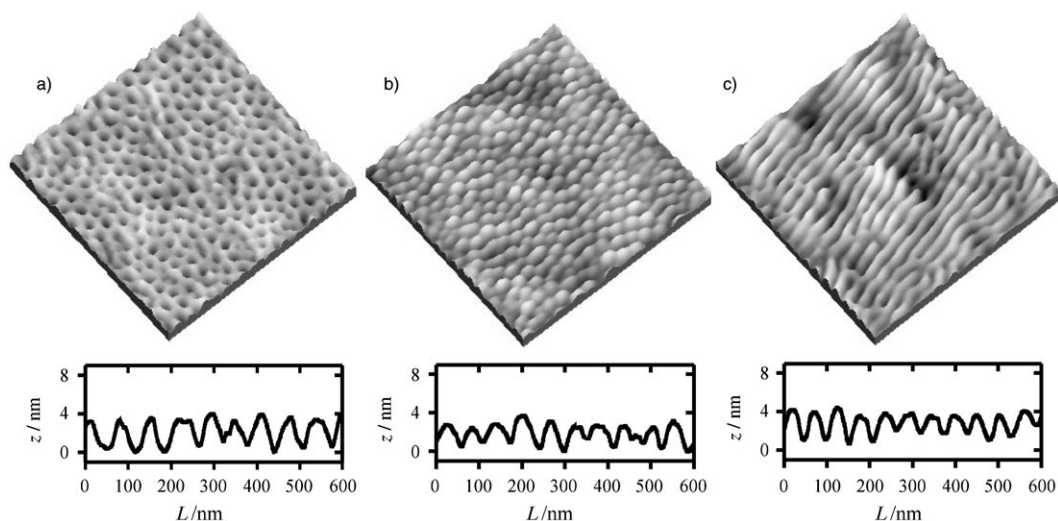
Figure 14. $1\times1\,\mu m^2$ AFM images (top) and cross sections (bottom) of a) dodecanethiolate-covered Au master; b) inner face of a Cu film after the release step. The film was electrodeposited at $j=10\,mA\,cm^{-2}$ from CuSO$_4$·5H$_2$O (0.6 M) + H$_2$SO$_4$ (0.5 M) + thiourea (0.025 mM), plating bath temperature $T=$ 25°C. c) inner face of a Cu film after the release step. The film was electrodeposited at $j=1\,mA\,cm^{-2}$ from the plating bath described in b).

similar images taken on the Au master. It means that some increase in roughness takes place during Cu deposition or during the release step. As the thickness of the dodecanethiolate SAMs on Au(111) is 1.7 nm the Cu nanocontacts broken during the release step could be responsible of the observed increase in roughness. The thickness of the alkanethiolate SAM introduces, then, the limit in the vertical resolution.

AES spectra taken for the dodecanethiolate-covered Au master before electrodeposition (Figure 15a) and after the release step (Figure 15b) shows similar S/Au ratios demonstrating that the alkanethiolate SAM remains adsorbed on the Au master during the complete procedure depicted in Figure 2. Similar results are obtained for Cu masters. This is an important issue because it implies that the same master can be used for several pattern transfer processes. On the

other hand, the surface of the patterned film is relatively free of impurities from the alkanethiolate layer as neither S nor C can be observed.

We have also varied the electrodeposition current in the range $1\,mA\,cm^{-2} \leq j \leq 20\,mA\,cm^{-2}$. For $j=10\,mA\,cm^{-2}$ the electrodeposition process results in good quality Cu dots. On the other hand, for $j < 5\,mA\,cm^{-2}$ the dot pattern transforms into well defined ripples 50 nm in size separated by 2 ± 0.5 nm in depth channels (Figure 14c). The transformation from dots to ripples was observed also on nanopatterned Au masters after annealing at 100°C suggesting that the surface mobility plays a key role in this transition.[42] It is possible that at low electrodeposition currents the Cu surface has enough time to rearrange into ripples that should exhibit a low surface free energy than the dotted surface. Therefore, by tuning the electrodepositon rate a variety of nanopatterns can be produced.

Finally, a comparison between the method and the well-known replica-molding technique[43] with polydimethylsiloxane (PDMS) should be made. While direct molding with PDMS stamps is applicable only to polymeric materials, the electrochemical nano/micropatterning method described in this work can be used as a technique for transferring surface–relief patterns on metals, alloys, oxides and also to conducting polymers. This technique merges the simplicity of the "soft lithographic" strategies[44] with the versatility of electrochemical deposition to synthesize a broad variety of materials, leading probably to the first example of an "electrochemical soft lithographic" technique.
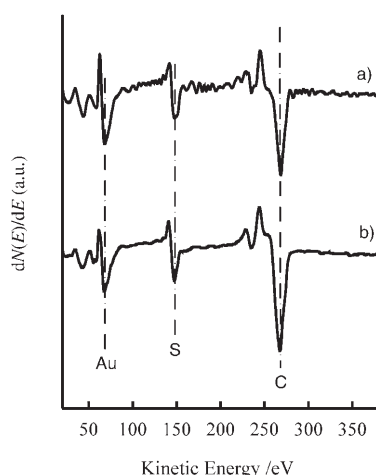

Figure 15. AES spectra taken for the dodecanethiolate-covered Au master a) before electrodeposition and b) after the release step. The Au, S and C signals are indicated.

Concluding Remarks and Outlook

Self-assembled monolayers can be used as key agents for pattern transfer with nanometer resolution. The electrochemical molding method based on SAMs is able to build

stable, three dimensional nano/microstructures in a simple and inexpensive way. The method allows molding/replication on metals and alloys in a single step/two step procedure by using techniques and equipments available for any chemistry laboratory.

Electrochemical molding can be used for preparing nano-patterned ultrathin metallic coatings on different materials. In fact, before the release step, the outer face of the electrodeposited metal films can be used as a substrate for electrodeposition of a foreign metal or alloy by simple changing the plating bath. In a similar way, the outer face of the electrodeposited film (before detachment from the master) can also be subjected to physical vapor deposition, chemical vapor deposition, reactive sputtering or simple polymer casting allowing deposition of a broad spectra of materials with controllable thickness. The release step from the master leaves a nanopatterned thin metallic coating placed on top of a foreign base material. Thus, nanopatterned metal coated ceramic, semiconductors and polymers films could be easily prepared. The possible application of the method for fabricating nanoclusters and nanocontacts on conducting substrates is another interesting field to be explored.

At present, the method has been applied to mold and to replicate rounded nano/microstructures with a relative low height/lateral size ratio (aspect ratio). The possibility to extent electrochemical nano/micropatterning to more complex architectures and higher aspect ratio should also be explored.

Finally, further in-depth investigations are required for improving SAM quality reducing the defect size and density, and accordingly increasing the lateral resolution of the method. In addition it is important to develop simple methods to produce good quality and stable SAMs on harder metals such as Ni. Harder metals are important to increase the life time of the molds that are subjected to wear during the deposition and release cycles.

Experimental Section

Self-assembled alkanethiolate monolayers were prepared from the liquid phase. In the case of Au and Ag surfaces the substrates were immersed for 24 h in 70 µм alkanethiolate containing ethanolic solutions. In the case of Cu surfaces alkanethiolates were self-assembled by immersion in 50 µм toluene containing solutions for 2 h. Electrochemical data for SAMs electrodesorption were made using either aqueous NaOH (0.1 м) or NaOH (0.1 м) + H_2O (5 %) in methanol as electrolyte at a scan rate of 0.05 V s^{-1}.

Metal electrodeposition was performed in a conventional three-electrode electrochemical cell using either the alkanethiolate-covered nano/micropatterned master as the working electrode, a large platinum sheet as counterelectrode, and a saturated calomel electrode as reference electrode. Potentials in the text are referred to the calomel saturated electrode.

Different plating baths were used. $Fe_{11}Co_{38}Ni_{51}$ electrodeposits were galvanostatically grown at $j = 20$ mA cm^{-2} from $CoSO_4\cdot7H_2O$ (0.06 м) + $NiSO_4\cdot6H_2O$ (0.2 м) + $FeSO_4\cdot7H_2O$ (0.015 м) + NH_4Cl (0.028 м) + H_3BO_3 (0.4 м) + thiourea (2.6×10$^{\cdot}$м), pH 2.8.[39] Cu_2O electrodeposition was performed under potentiostatic conditions at $E = -0.45$ V from $CuSO_4\cdot5H_2O$ (0.4 м) + lactic acid (3 м) pH 9 at $T = 60$ °C.[40] Cu electro-

deposition was made under galvanostatic conditions with j ranging from 1 mA cm^{-2} to $j = 10$ mA cm^{-2} from $CuSO_4\cdot5H_2O$ (0.6 м) + H_2SO_4 (0.5 м) + thiourea (0.025 mм) plating bath at $T = 25$ °C.[4]

After electrodeposition, the respective films (metals and alloys) were released from the master by using small tweezers (as those used for handling microscope samples). We have verified that this procedure introduces no damages neither on the patterned nor on the master. In the case of Cu_2O samples due to the brittle characteristics of the ceramic film, release from the master by using small tweezers is not recommended. In some cases the thin sample can be damaged by exerting excessive pressure with the tweezers tips. One safer way to release the micromolded Cu_2O sample is releasing the deposited film by using a Scotch tape or by gluing the Cu_2O deposit to a glass substrate and then easily releasing from the master while holding the glass substrate with small tweezers.

All the electrolytes were degassed with purified nitrogen for 2 h before the electrochemical runs. STM (constant current) and AFM (contact mode) images were taken with a Nanoscope III (Digital Instruments, Santa Barbara CA) using Pt/Ir and Si_3N_4 tips, respectively. Finally, the elemental surface chemical composition of the deposited films was determined by Auger Electron Spectroscopy (AES) using a single pass cylindrical mirror analyzer (CMA, Physical Electronics).

[1] G. Timp in *Nanotechnology*, Springer, New York, **1999**.
[2] Y. Xia, J. A. Rogers, K. E. Paul, G. M. Whitesides, *Chem. Rev.* **1999**, *99*, 1823; B. H. Gates, Q. Xu, M. Stewart, D. Ryan, G. Wilson, G. M. Whitesides, *Chem. Rev.* **2005**, *105*, 1171.
[3] R. W. Jaszewski, H. Schift, B. Schnyder, A. Schneuwly, P. Gröning, *Appl. Surf. Sci.* **1999**, *143*, 301; S. Zhang, X. Zeng, Z. Tang, M. J. Tan, *Int. J. Mod. Phys. B* **2002**, *16*, 1080.
[4] P. L. Schilardi, O. Azzaroni, R. C. Salvarezza, *Langmuir* **2001**, *17*, 2748.
[5] O. Azzaroni, M. Fonticelli, G. Benítez, P. L. Schilardi, R. Gago, I. Caretti, L. Vázquez. , R. C. Salvarezza, *Adv. Mater.* **2004**, *16*, 405.
[6] L. Vázquez, R. C. Salvarezza, A. J. Arvia, *Phys. Rev. Lett.* **1997**, *79*, 709.
[7] A. Ulman, *Chem. Rev.* **1996**, *96*, 1533; J. A. Love, L. A. Estroff, J. K. Kriebel, R. G. Nuzzo, G. M. Whitesides, *Chem. Rev.* **2005**, *105*, 1103.
[8] F. Schreiber, *Prog. Surf. Sci.* **2000**, *65*, 151, and references therein.
[9] O. Azzaroni, P. L. Schilardi, R. C. Salvarezza, *Nano Lett.* **2001**, *1*, 291.
[10] T. Baunach, V. Ivanova, D. M. Kolb, H.-G. Boyen, P. Ziemann, M. Büttner, P. Oelhafen, *Adv. Mater.* **2004**, *16*, 2024.
[11] a) G. Benítez, C. Vericat, S. Tanco, F. Remes Lenicov, M. F. Castez, M. E. Vela, R. C. Salvarezza, *Langmuir* **2004**, *20*, 5030; b) C. Vericat, G. Andreasen, M. E. Vela, H. Martín, R. C. Salvarezza, *J. Chem. Phys.* **2001**, *115*, 6672.
[12] M. A. Auger, P. L. Schilardi, I. Caretti, O. Sanchez, G. Benítez, J. M. Albella, R. Gago, M. Fonticelli, L. Vazquez, R. C. Salvarezza, O. Azzaroni, *Small* **2005**, *3*, 300.
[13] O. Azzaroni, P. L. Schilardi, R. C. Salvarezza, J. M. Herrero, C. Zaldo, L. Vazquez unpublished results.
[14] J. A. Switzer, C.-J. Hung, E. W. Bohannan, M. G. Shumsky, T. D. Golden, D. C. VanAken, *Adv. Mat.* **1997**, *4*, 334; F. Y. Yang, K. Liu, K. Hong, D. H. Reich, P. C. Searson, C. L. Chien, *Science* **1999**, *284*, 1335; J. A. Switzer, M. J. Shane, R. P. Phillips, *Science* **1990**, *247*, 444; J. A. Switzer, M. G. Shumsky, E. W. Bohanna, *Science* **1999**, *284*, 293.

[15] H. Ron, H. Cohen, S. Matlis, I. Rubinstein, *J. Phys. Chem. B* **1998**, *102*, 986115.

[16] M. E. Castro, J. M. White, *Surf. Sci.* **1991**, *257*, 22.

[17] M. Stratmann, *Adv. Mater.* **1990**, *29*, 191.

[18] Z. Mekhalif, A. Lazarescu, L. Hevesi, J.-J. Pireaux, J. Delhalle, *J. Mater. Chem.* **1998**, *8*, 545; Z. Mekhalif, J. Riga, J.-J. Pireaux, J. Delhalle, *Langmuir* **1997**, *13*, 2285.

[19] G. E. Poirier, M. J. Tarlov, *J. Phys. Chem.* **1995**, *99*, 10966.

[20] S. Sohn, M. Schröder, D. Lipinsky, H. F. Arlinghaus, *Surf. Interface Anal.* **2004**, *36*, 1222.

[21] C. A. Widrig, C. Chung, M. D. Porter, *J. Electroanal. Chem.* **1991**, *310*, 335; M. M. Walczak, C. Chung, S. M. Stole, C. A. Widrig, M. D. Porter, *J. Am. Chem. Soc.* **1991**, *113*, 2370.

[22] H. H. Hagenströmg, M. Schneeweiss, D. M. Kolb, *Langmuir* **1999**, *15*, 2435.

[23] D. W. Hatchett, R. H. Uibel, K. J. Stevenson, J. M. Harris, H. S. White, *J. Am. Chem. Soc.* **1998**, *120*, 1062.

[24] O. Azzaroni, M. E. Vela, M. Fonticelli, G. Benítez, P. Carro, B. Blum, R. C. Salvarezza, *J. Phys. Chem. B* **2003**, *107*, 13446.

[25] T. Kondo, T. Sumi, K. Uosaki, *J. Electroanal. Chem.* **2002**, *538–539*, 59.

[26] H. Munakata, D. Oyamatsu, S. Kuwabata, *Langmuir* **2004**, *20*, 10123.

[27] M. Esplandiu, H. Hagenströmg, *Solid State Ionics* **2002**, *150*, 39.

[28] D. J. Lavrich, S. M. Wetterer, S. L. Bernasek, G. Scoles, *J. Phys. Chem. B* **1998**, *102*, 3456.

[29] O. Azzaroni, P. L. Schilardi, R. C. Salvarezza, *Electrochim. Acta* **2003**, *48*, 3107.

[30] S. Darby, T. V. Mortimer-Jones, R. L. Johnson, C. Roberts, *J. Chem. Phys.* **2002**, *116*, 1536.

[31] O. Azzaroni, M. Cipollone, M. E. Vela, R. C. Salvarezza, *Langmuir* **2001**, *17*, 1483.

[32] A. Ghatak, K. Vorvolakos, H. She, D. L. Malotky, M. K. Chaudhury, *J. Phys. Chem. B* **2002**, *104*, 4018.

[33] B.-M. Zhang Newby, M. J. Chaudhury, H. R. Brown, *Science* **1995**, *269*, 1407.

[34] J. P. Lee, Y. J. Jang, M. M. Sung, *Adv. Funct. Mater.* **2003**, *13*, 873.

[35] G. Andreasen, P. L. Schilardi, O. Azzaroni, R. C. Salvarezza, *Langmuir* **2002**, *18*, 10430.

[36] A.-L. Barabasi, H. E. Stanley, *Fractal Concepts in Surface Growth*, Cambridge University Press, Cambridge **1995**; F. Family, T. Vicsek, *J. Phys. A* **1985**, *18*, L75.

[37] A. De Virgiliis, O. Azzaroni, R. C. Salvarezza. E. V. Albano, *Appl. Phys. Lett.* **2003**, *82*, 1953.

[38] P. F. de Leon, E. V. Albano, H. Solari, R. C. Salvarezza, *Phys. Rev. E* **2002**, *66*, 042601(1).

[39] O. Azzaroni, P. L. Schilardi, R. C. Salvarezza, *Appl. Phys. Lett.* **2002**, *80*, 1061.

[40] T. Osaka, T. Sawaguchi, F. Mizutani, T. Yokoshima, M. Takai, Y. Okinaka, *J. Electrochem. Soc.* **1999**, *146*, 3295.

[41] Y. C. Zhou, J. A. Switzer, *Scripta Mater* **1998**, *38*, 1731.

[42] C. Alonso, R. C. Salvarezza, J. M. Vara, A. J. Arvia, *Electrochim. Acta* **1990**, *35*, 1131.

[43] Y. Xia, J. J. McClelland, R. Gupta, D. Qin, X.-M Zhao, L. L. Sohn, R. J. Celotta, G. M. Whitesides, *Adv. Mater.* **1997**, *9*, 147.

[44] Y. Xia, G. M. Whitesides, *Angew. Chem.* **1998**, *110*, 568; *Angew. Chem. Int. Ed.* **1998**, *37*, 550.